



OPEN ACCESS

EDITED BY

Warangkana Srichamnong,
Mahidol University, Thailand

REVIEWED BY

Consolatina Liguori,
University of Salerno, Italy
Luiz Colnago,
Embrapa Instrumentacao, Brazil
William S. Price,
Western Sydney University, Australia

*CORRESPONDENCE

Gisela Guthausen,
✉ gisela.guthausen@kit.edu

RECEIVED 14 September 2023

ACCEPTED 29 November 2023

PUBLISHED 03 January 2024

CITATION

Trapp L, Kafashian S, Schacht H, Nirschl H and Guthausen G (2024), Quality control of hazelnut-based spreads: ^1H TD-NMR transverse relaxation.
Front. Food. Sci. Technol. 3:1294332.
doi: 10.3389/frfst.2023.1294332

COPYRIGHT

© 2024 Trapp, Kafashian, Schacht, Nirschl and Guthausen. This is an open-access article distributed under the terms of the [Creative Commons Attribution License \(CC BY\)](https://creativecommons.org/licenses/by/4.0/). The use, distribution or reproduction in other forums is permitted, provided the original author(s) and the copyright owner(s) are credited and that the original publication in this journal is cited, in accordance with accepted academic practice. No use, distribution or reproduction is permitted which does not comply with these terms.

Quality control of hazelnut-based spreads: ^1H TD-NMR transverse relaxation

Lena Trapp¹, Saghar Kafashian¹, Hilke Schacht², Hermann Nirschl¹ and Gisela Guthausen^{1,3*}

¹Institute of Mechanical Process Engineering and Mechanics, Karlsruhe Institute of Technology, Karlsruhe, Germany, ²Fraunhofer Institute for Process Engineering and Packaging IVV, Freising, Germany, ³Engler-Bunte-Institut, Water Chemistry and Technology, Karlsruhe Institute of Technology, Karlsruhe, Germany

Hazelnut-based spreads are very popular, and they are available in a variety of compositions and prices. They, therefore, require detailed quality control and reliable fraud detection regarding the substitution of high-cost cocoa butter. Transverse relaxation measured via ^1H time domain NMR (TD-NMR) is an approach that is compatible with industrial quality control but allows an in-depth insight into the materials. When transverse relaxation is measured as a function of temperature in a moderate range $T \in [253, 353]$ K, the melting of cocoa butter and palm oil can be studied. The observations can be taken as a basis for quality control as the prices of these two components are significantly different. Fats introduce different qualities to the spreads in addition. This paper describes the experimental procedure and the findings on a spread sample basis with a considerable span width regarding the ingredients of commercially available hazelnut-based spreads.

KEYWORDS

^1H -NMR, R_2 -relaxation, TD-NMR, hazelnut-based spread, quality control, food fraud detection

1 Introduction

Product fraud is a well-known problem in a wide range of industries. Apart from branded clothing and cosmetics, criminals are not stopping at adulterated food products (Ulberth and Buchgraber, 2000). Food fraud is often motivated by raw material costs to maximize financial profit. Popular examples of adulterated foods are olive oil, honey, wine, coffee, and fruit juices (Cordella et al., 2002; Ogrinc et al., 2003; Santos et al., 2016; Santos et al., 2017; Siddiqui et al., 2017). The adulterants usually do not pose a health risk to the consumer. The consumer, however, is deceived with respect to the quality, origin, and physiological value of the food, thus violating the consumer's basic rights. Efficient food control procedures are indispensable due to these criminal intentions. Analytical techniques should provide reliable quality parameters that can be easily and reproducibly measured. A standard operating procedure (SOP) ensures that the method functions independently from the user. In addition, fast and cost-efficient measurement procedures are preferred. Nuclear magnetic resonance (NMR) represents a powerful and non-destructive device that is well-established in the food environment and also in the detection of adulteration. Apart from high-resolution NMR spectroscopy, the cost-efficient ^1H time domain NMR (TD-NMR) with low-field instruments is widely spread in the food industry for quality control (Hills, 2006; van Duynhoven et al., 2010; Meyer et al., 2016; Blümich, 2019; Ezeanaka et al., 2019). Measurements of transverse relaxation provide information about the intrinsic molecular

mobility in the low-frequency range. Since the transverse relaxation rate R_2 of substances (e.g., water, oil, and fat) differs, the composition of samples is accessible not only by NMR-spectra but also with integral relaxation measurements by TD-NMR. To establish such a method, extensive preliminary investigations are necessary in both high-field and low-field NMR to find suitable parameters that allow conclusions to be drawn about the constituents of the samples.

Nut spreads are frequently consumed and, therefore, represent an important market segment for food products. Nut spreads are dispersions of solids in oils or fats derived from mostly hazelnuts and other drupes. A creamy, spreadable mass is available at room temperature due to the partial crystallization of high-melting triglycerides, which are mainly found in solid fats such as palm oil (PO) and cocoa butter (CB). A large proportion of the solids are finely ground nuts, sugar, milk powder, and cocoa powder. Commercial nut spreads are available in supermarkets in a huge variety of recipes but also fineness, homogeneity, and viscosity (Principato et al., 2022). PO is often added to nut spreads as a fatty phase to give the product a creamy consistency and stability. Due to the currently discussed ecological problems in PO production, alternative structuring fats come into the focus of the food industry and recipe development (Kovács et al., 2021; Marra et al., 2023). Some products are already constituted with CB instead of PO. However, the substitution of PO is associated with considerably higher raw material costs, changed physical parameters, and taste (Aydemir, 2019), and thus invites food fraud. For example, with a price of \$830 per ton in September 2023 (World Bank, 2023), PO is nearly five to 10 times cheaper than CB. A suitable analytical method is, therefore, highly desirable. To the best of our knowledge, no analytical approach exists so far to detect possible frauds in nut-based spreads in a fast, non-destructive, and convenient way with good reproducibility. In this paper, we describe the use of the multi-echo sequence CPMG (Carr, Purcell, Meiboom, Gill) for that purpose and provide evidence for its suitability.

The aim of this study was to show the suitability of TD-NMR for the discrimination of PO- and CB-containing nut spreads and thus provide a basis for fraud detection in the context of hazelnut-based spreads. The NMR transverse relaxation properties of nut spreads were investigated to find reliable and well-defined quality characteristics with a focus on easily, but reliably, measurable parameters. Spectrally resolved measurements provided the basis for a TD-NMR application. Temperature-dependent measurements with TD-NMR provide insights into fat melting and allow for differentiation of the spreads. Measurements were performed on 20 commercially available hazelnut-based spreads and five fat raw materials as reference samples: hazelnut oil (HNO), sunflower oil (SFO), rapeseed oil (RO), PO, and CB.

2 Materials and methods

2.1 Materials

Virgin HNO was obtained from Reichold Feinkost GmbH (Diez, Germany), SFO from Nestlé (Vevey and Cham, Switzerland), RO from RAPSO Österreich GmbH (Aschach an der Donau, Austria), PO from Landkrone Naturkost und Naturwaren GmbH (St. Ingbert,

Germany), and CB from Alnatura Produktions-und Handels GmbH (Darmstadt, Germany) as the main fat components of nut spreads. Because of the high content of unsaturated fatty acids, HNO (95% (Crews et al., 2005)), SFO (91% (Chowdhury et al., 2007)), and RO (93% (Lewinska et al., 2015)) are liquid at room temperature compared to CB (36%–43% (Naik and Kumar, 2014; Ghazani and Marangoni, 2021)) and PO (53% (Chowdhury et al., 2007)). In total, 20 hazelnut-based spreads (sample a-u, Table 1) were purchased from local supermarkets.

The samples were selected to cover a wide range of formulations. It is common to all spreads that their main components are sugar, vegetable oils or fats, cocoa, hazelnuts, and milk components (Table 2). The details of formulation and even of composition or fractions of the main ingredients are not disclosed to the consumer. All samples were stored at room temperature for weeks before the measurements, and melting was observed by transverse relaxation.

2.2 Instrumentation and NMR experiments

^1H -NMR spectroscopy and transverse relaxation measurements with spectral resolution were performed on an AVANCE NEO NanoBay 300-MHz spectrometer equipped with a broadband BBFO probe and the acquisition software package TopSpin 4.0.9 (Bruker, Ettlingen, Germany) at a temperature $T = 298\text{ K}$. The CPMG multi-echo sequence according to Carr, Purcell, and Meiboom and Gill (1958) was used (Figure 1). In addition, CPMG transverse relaxation measurements were performed on a 20 MHz time domain Bruker minispec mq20 instrument to investigate transverse relaxation as the potential quality control parameter. T was varied in 5 K steps between 298 K and 373 K. A holding time of 10 min preceded each NMR measurement, guaranteeing isothermal conditions spatially and temporally. The samples were filled into 5-mm (300 MHz) and 10-mm (20 MHz) NMR glass tubes with a filling height of 10 mm to reduce temperature gradients and therefore convection especially at elevated T . All samples were measured undiluted to explore the capabilities of TD-NMR on samples, as available in quality control.

The main NMR parameters are listed in Table 3.

2.3 Data processing

Pseudo-2D datasets were recorded on the AVANCE NEO NanoBay 300-MHz spectrometer. Pseudo-2D means, in this context, that one dimension of the dataset is a time scale, $n \cdot \tau_e$ (τ_e being the echo time and n the number of the echo), and the other dimension is the free induction decay (FID) time scale. The data were Fourier-transformed along that dimension and phase-corrected, providing chemical shift information (Figure 2). The waterfall plot shows largely unstructured spectra due to mainly homonuclear dipolar interactions. The spectra do not allow for an in-detail chemical analysis of fat composition. This would require either dissolution of the fats at a low concentration and measurements with dedicated pulse sequences or higher temperatures, leading to a comparison with spectra in the literature and databases (Díaz et al., 2005; Trapp et al., 2023).

TABLE 1 Ingredients as reported on the label packaging of the 20 commercial nut spreads.

Sample	Ingredients
a	Sugar, cocoa butter , hazelnuts, skimmed milk powder, cocoa (17%), sunflower oil, safflower oil , rice oil , sunflower fat, coconut fat , almonds , and emulsifier: lecithin and vanilla
b	Sugar, cocoa butter , rapeseed oil, hazelnuts (14%), defatted cocoa (11%), dried rice syrup , emulsifier: lecithin, butter fat, soy fiber (3%), and flavors
c	Cane sugar, cocoa butter , hazelnuts (13%), skimmed milk powder, defatted cocoa (8.5%), sunflower oil, and emulsifier: lecithin
d	Cane sugar, cocoa butter , hazelnuts (30%), skimmed milk powder, defatted cocoa, dried rice syrup , sunflower oil, and emulsifier: lecithin
e	Sugar, cocoa butter , rapeseed oil (25%), sweet whey powder, hazelnut mass (5%), skimmed milk powder, defatted cocoa, sunflower oil, and emulsifier: lecithin, salt, and flavors
f	Sugar, cocoa butter , sweet whey powder, hazelnuts (20%), skimmed milk powder, lactose , defatted cocoa (7%), sunflower oil, and emulsifier: lecithin
g	Cane sugar, cocoa butter , hazelnuts (18%), roasted and chopped hazelnuts (4%), skimmed milk powder, defatted cocoa, sunflower oil, emulsifier: lecithin, and vanilla
h	Cane sugar, cocoa butter (6.5%), hazelnuts (18.5%), skimmed milk powder, defatted cocoa, sunflower oil, emulsifier: lecithin, and vanilla
i	Cocoa butter , hazelnuts (33%), cocoa, sunflower oil, and xylitol
j	Sugar, cocoa butter , rapeseed oil, shea nut oil , sweet whey powder, hazelnut mass (14%), skimmed milk powder, lactose , defatted cocoa, wheat flour, sunflower oil, emulsifier: lecithin, butter fat, leavening agent, salt, and flavors (with chocolate biscuit crumbs and crispy brittle)
k	Sugar, cocoa butter , corn starch , sweet whey powder, hazelnuts (13%), skimmed milk powder, defatted cocoa (9%), sunflower oil, emulsifier: lecithin, and maltodextrin
l	Sugar, palm oil , hazelnuts (13%), skimmed milk powder (8.7%), defatted cocoa, emulsifier: lecithin, and vanilla
m	Sugar, palm oil , hazelnuts (13%), skimmed milk powder (5.5%), defatted cocoa (3.7%), almonds , and emulsifier: lecithin
n	Cane sugar, palm oil , hazelnuts (14%), defatted cocoa, sunflower oil, vanilla, and sweet lupine flour
o	Cane sugar, palm oil , hazelnuts (13%), skimmed milk powder, defatted cocoa (7%), sunflower oil, and vanilla
p	Sugar, palm oil , rapeseed oil, hazelnuts (13%), skimmed milk powder (7.5%), defatted cocoa (7.5%), emulsifier: lecithin, and lactase
q	Cane sugar, palm oil , hazelnuts (45%), skimmed milk powder (10%), defatted cocoa (4%), and vanilla
r	Cane sugar, palm oil , hazelnuts (15%), defatted cocoa (9%), sunflower oil, emulsifier: lecithin, and vanilla
s	Sugar, palm oil , rapeseed oil, hazelnuts (13%), skimmed milk powder, defatted cocoa (9%), sunflower oil, and emulsifier: lecithin
t	Sugar, palm oil , rapeseed oil, sweet whey powder, hazelnuts, skimmed milk powder (2.5%), defatted cocoa (6.5%), and emulsifier: lecithin (inhomogeneous distribution of defatted cocoa (black–white pattern))

TABLE 2 Typical ranges of mass fractions of the main components in commercial nut spreads.

	Sugar	Vegetable oils	Hazelnut	Milk ingredients	Cocoa
%	[2.1, 57]	[28, 53]	[5, 45]	[5.5, 11]	[3.7, 9]

The normalized signal attenuation SS_0^{-1} of the designed regions (unitless) was plotted as a function of $n \cdot \tau_c$, showing the magnetization decays (Figure 3). The signal decays of the three integration areas show identical time dependence within the experimental error and are discussed in more detail in Section 3.1.

As the decays are independent of the chemical shift, the signal can be measured integrally without loss of information as it is usually done in TD-NMR. The echo maxima S were recorded as an average over a few data points for each echo as a function of $n \cdot \tau_c$ (Figure 1). These TD-NMR ^1H relaxation curves were normalized to the signal amplitude of the first echo S_0 and analyzed via fits of Eqs 1, 2 using Origin software, version 2021 (OriginLab Corporation, Northampton, United States), using the Levenberg–Marquardt

algorithm. The coefficient of determination R^2 was always larger than 99%.

Nut spreads and raw oils and fats cannot be regarded as “simple” spin systems, which is already evident from their chemical composition and additionally motivated by the state of aggregation of the components. Thus, magnetization decays differ from a mono-exponential decay function which would be expected for liquid and often diluted small molecules. To extract interesting material parameters, the measured decays were further condensed by modeling the decays with gamma distributions (Förster et al., 2017), which allows the extraction of the mean value and the distribution width of the transverse relaxation rates. The mean transverse relaxation rate $\langle R_2 \rangle$ and the associated distribution

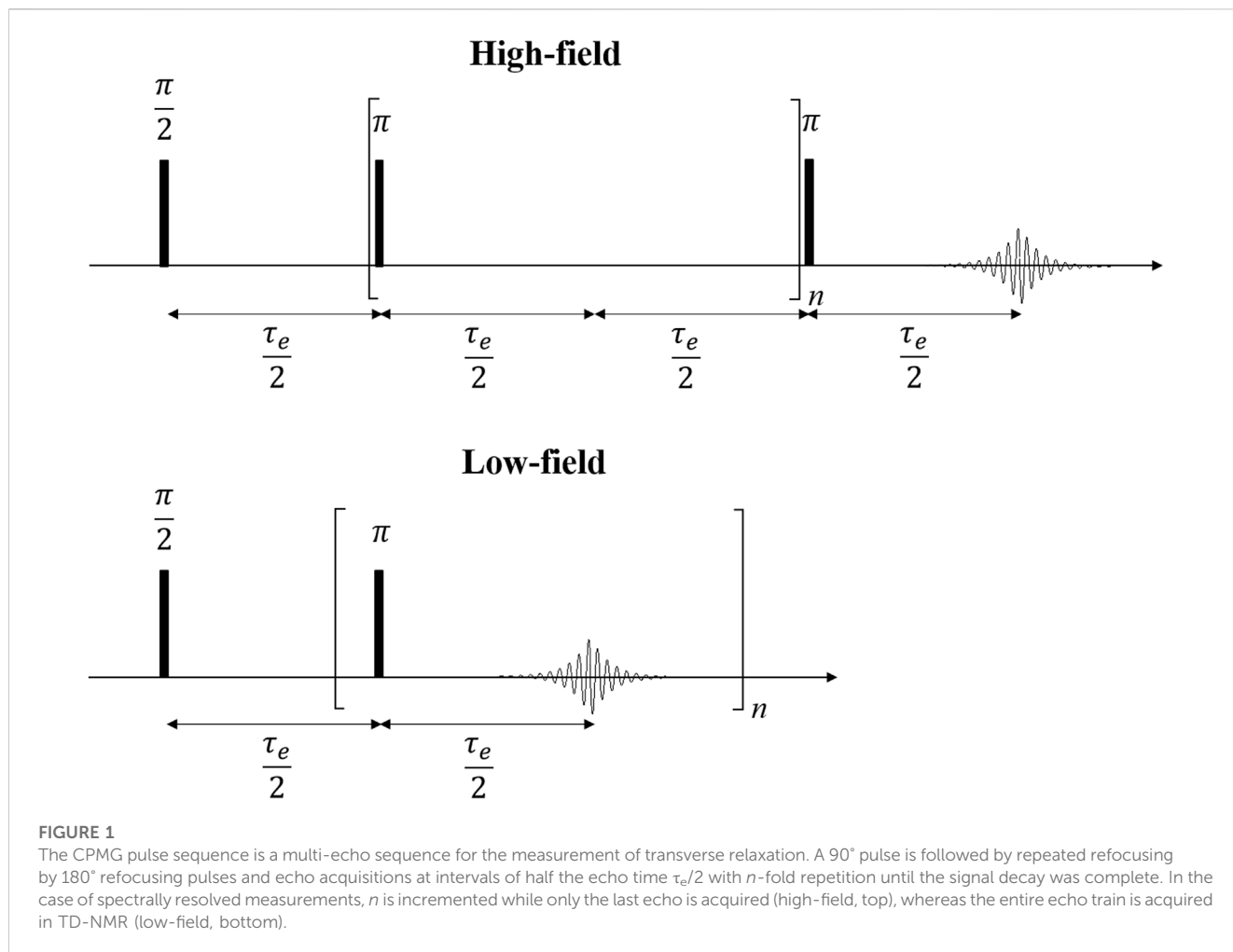


TABLE 3 Main parameters of the ¹H-NMR experiments.

	Single pulse (300 MHz)	CPMG (300 MHz)	CPMG (20 MHz)
Number of averages [-]	8	8	8
Number of acquired echoes [-]	-	32	1,500
Acquired data points per spectrum [-]	8,192	8,192	-
Repetition time t_R [s]	4	4	5
Echo time τ_e [ms]	-	1.2	2
Temperature T [K]	298	298	[298, 373]
Measurement time [min]	1	19	1

width σ were derived from the NMR raw data, according to the following equation:

$$\frac{S}{S_0} = \left(1 + n \cdot \tau_e \cdot \frac{\sigma^2}{\langle R_2 \rangle} \right)^{-\frac{\langle R_2 \rangle^2}{\sigma^2}} \quad (1)$$

A bimodal distribution is required to describe numerically well the magnetization decays of fats and multicomponent blends such as

hazelnut-based spreads at temperatures below the melting temperatures $T < T_M$:

$$\frac{S}{S_0} = A_1 \left(1 + n \cdot \tau_e \cdot \frac{\sigma_1^2}{\langle R_{2,1} \rangle} \right)^{-\frac{\langle R_{2,1} \rangle^2}{\sigma_1^2}} + A_2 \left(1 + n \cdot \tau_e \cdot \frac{\sigma_2^2}{\langle R_{2,2} \rangle} \right)^{-\frac{\langle R_{2,2} \rangle^2}{\sigma_2^2}} \quad (2)$$

The amplitudes A_i and the relaxation parameters $\langle R_{2,i} \rangle$ and σ_i were determined by non-linear least squares fits. The fit parameters

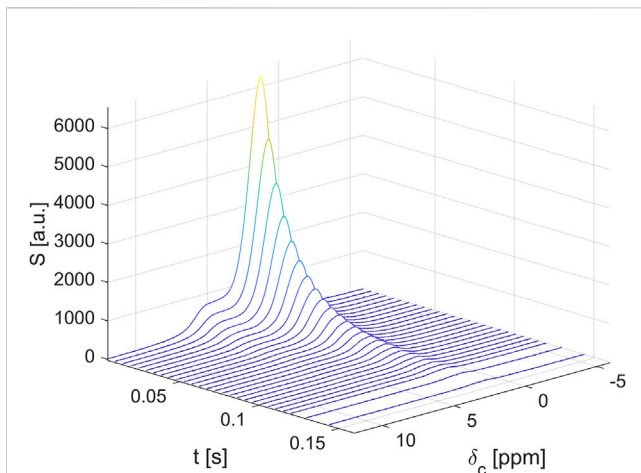


FIGURE 2

The spectrally resolved transverse relaxation at 300 MHz on a hazelnut-based spread shows a continuous decay independent of the chemical shift, apart from the significant line broadening.

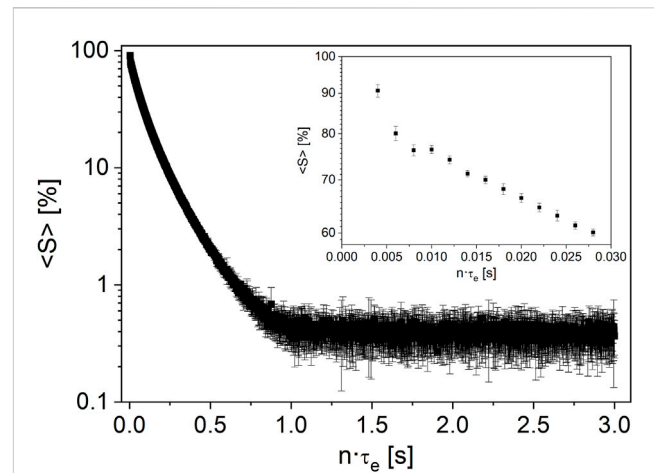


FIGURE 4

Mean measured signal $\langle S \rangle$ in a repeated CPMG experiment at 20 MHz on a nut spread at room temperature. The error bars indicate the calculated standard deviation of each measured echo over 10 repetitions. The noise level scatters by less than 1% absolute; the first echoes with the largest signal intensity in the inset show an absolute scatter below 2%.

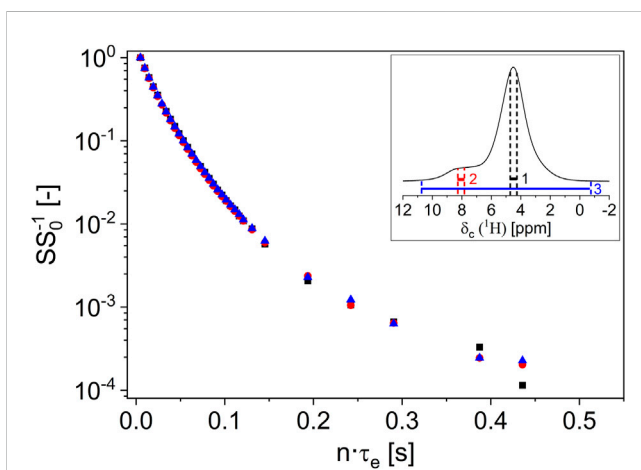


FIGURE 3

The normalized transverse signal decays at 300 MHz of the two broad main signal regions 1 (inset, black region) and 2 (inset, red region) on a hazelnut-based spread show identical transverse relaxation behavior down to the noise level. An integral (inset, blue region) measurement of the transverse relaxation is, therefore, appropriate. The curvature of magnetization in the semi-log graph indicates a distribution of relaxation rates.

provide detailed insights into the relaxation behavior of the spreads and will be discussed in the context of quality control and fraud detection.

2.4 Statistical validity

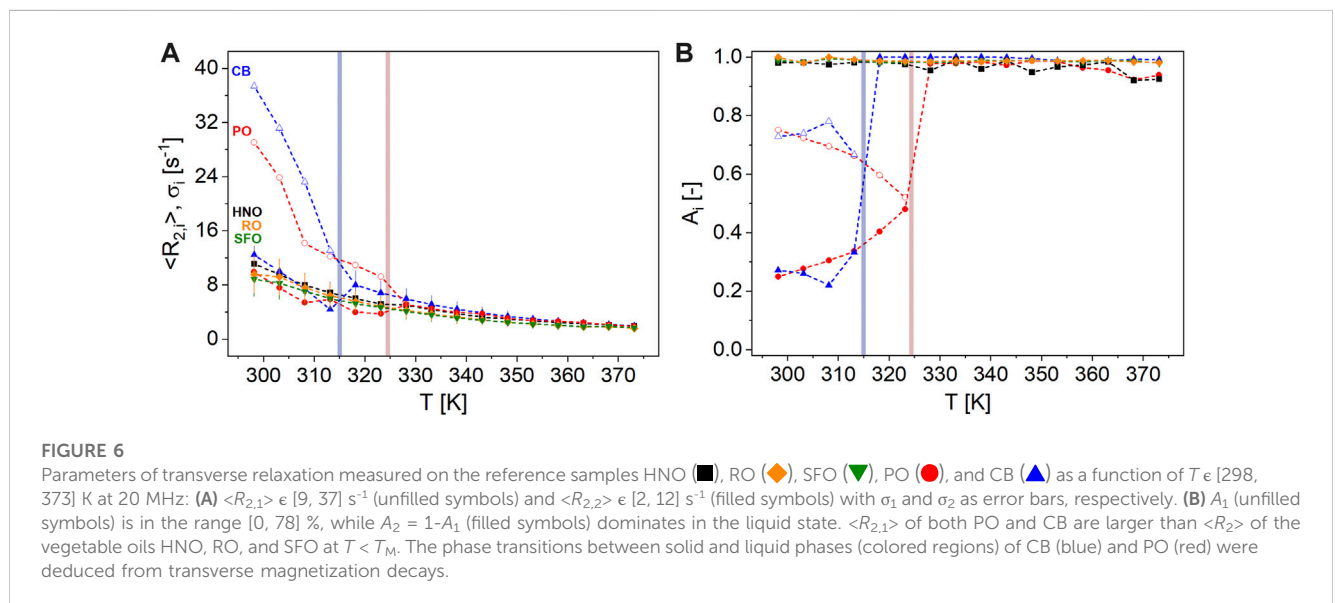
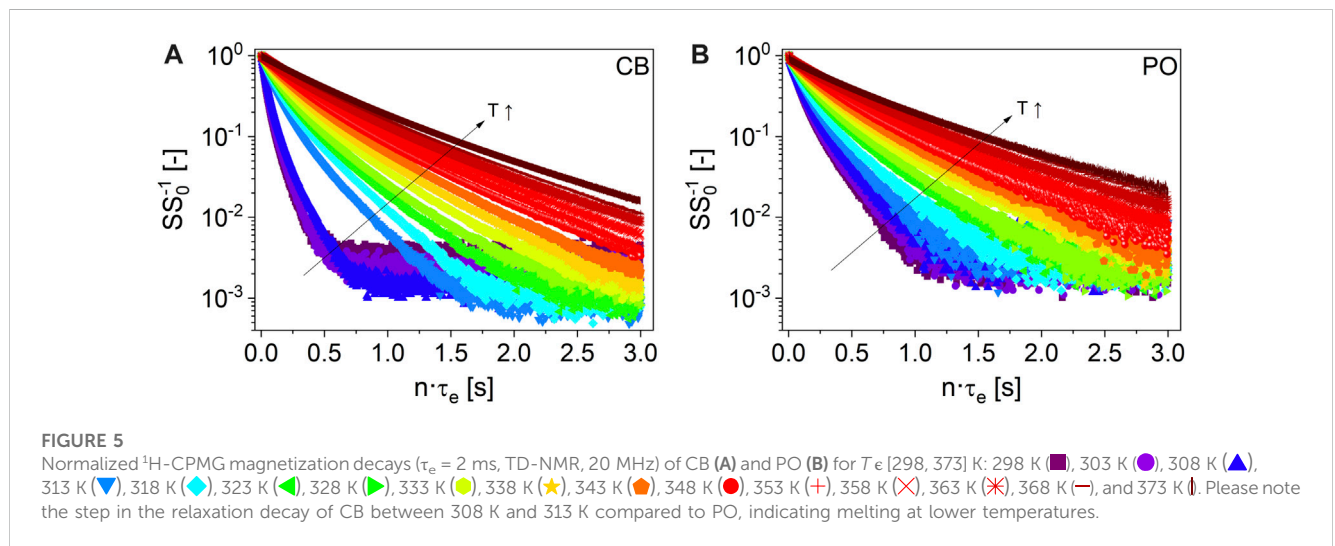
In quality control, the meaningfulness of sample preparation, raw data, and processing errors need to be known to be able to grade an analytical tool. The repeatability of a typical TD-CPMG measurement was, therefore, measured by investigating a single nut spread under worst-case conditions, i.e., measurements at room temperature, on a sample containing PO, taking 10 measurements

on the same sample tube to detect the error of the instrument (case A). In addition, the sampling error was investigated by filling and measuring 10 independently prepared samples of the same nut spread (case B).

The mean value of the measured data points (Figure 4) and the standard deviations of each data point in a low-field CPMG were deduced for cases A and B. The sample temperature was room temperature, which is a worst-case scenario: The permanent magnet was thermostated at 308 K with a potential impact on the sample temperature, which should be constant at 293 K. A probe was used which compensates this effect of temperature gradient at least partially; this high-temperature probe allows for measurements in the temperature range [173, 473] K as it is equipped with a vacuum-isolated glass dewar with the drawback that the radio frequency coil is much larger in diameter than the optimum diameter at approximately 12 mm for a 10-mm sample. The sensitivity of this probe is, therefore, lower than that of a non-thermostated probe. The vendor specification of a reproducibility of 5% of an NMR signal is met over the complete time scale of the CPMG measurement (Figure 4, case A); the observed values are significantly smaller than the specification. For case A, the statistical error in the time range $n \cdot \tau_e > 1$ s is less than 1%, measured as the absolute standard deviation of the raw signal; it amounts to a maximum of 2% measured as the relative error for $n \cdot \tau_e < 1$ s. For the reproducibility of sampling (case B), the errors are similar; the relative error for $n \cdot \tau_e < 1$ s amounted to 4%. Sample preparation induces, therefore, an additional error, as expected. In addition, the errors induced by data processing were quantified for both cases. As expected, modeling leads to additional statistical and systematic errors (Table 4). The mean relaxation rates show a relative error of the standard deviations of 4% ($\langle R_{2,1} \rangle$) and 5% ($\langle R_{2,2} \rangle$), while the relative error of the amplitudes is approximately 4% (A_1) and 10% (A_2) for case A. For case B, the relative errors are slightly larger.

TABLE 4 Reproducibility of the measured NMR parameters deduced from CPMG measurements at 20 MHz on nut spreads. The model used was the bimodal gamma distribution model, leading to the mean relaxation rates, the width of the distributions, and their amplitudes. Ten NMR measurements were performed on the same sample to determine the measurement error of the instrument (case A). To determine the additional error introduced by sample preparation, 10 samples of the same nut spread were prepared and measured (case B). Different nut spreads were used for cases A and B, and the absolute values, therefore, differ slightly.

Parameter	$\langle R_{2,1} \rangle$ [s ⁻¹]	σ_1 [s ⁻¹]	$\langle R_{2,2} \rangle$ [s ⁻¹]	σ_2 [s ⁻¹]	A ₁ [-]	A ₂ [-]
A) Errors in raw data and data treatment						
Mean value	16.0	2.5	4.9	0.6	0.7	0.3
Standard deviation	0.7	0.2	0.3	0.1	0.03	0.03
Relative error [%]	4.2	9.5	5.5	16.9	3.6	9.6
B) Errors in sample preparation, raw data, and data treatment						
Mean value	18.1	1.9	5.4	0.4	0.8	0.2
Standard deviation	0.9	0.2	0.4	0.04	0.03	0.03
Relative error [%]	5.1	10.3	7.4	11.0	3.2	13.0



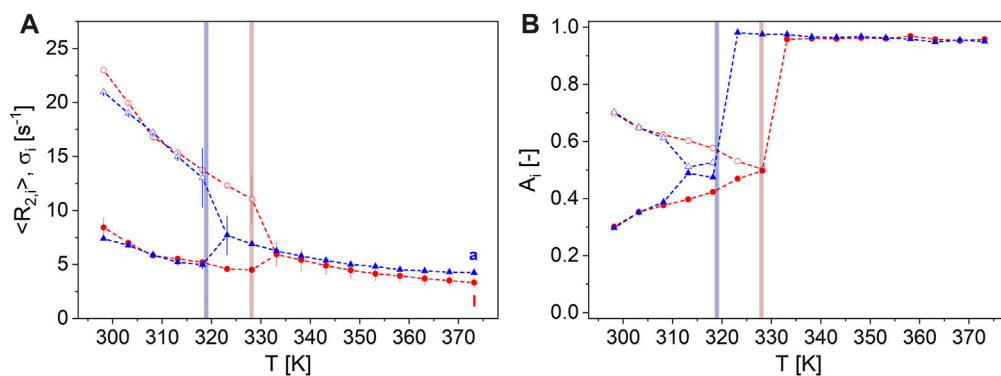


FIGURE 7

Magnetization decays at 20 MHz of two exemplary spreads were modeled by monomodal gamma distributions for large T , whereas at lower T , the bimodal description was appropriate. **(A)** The fast relaxing component is given by the mean value of distributions $\langle R_{2,1} \rangle \in [11, 24] \text{ s}^{-1}$ (unfilled symbols) and the slower component by $\langle R_{2,2} \rangle \in [3, 11] \text{ s}^{-1}$ (filled symbols) with σ_1 and σ_2 as the corresponding distribution widths (error bars). **(B)** A_1 (unfilled symbols) in the range [0, 70] % and $A_2 = 1 - A_1$ (filled symbols) of the nut spread samples a (\blacktriangle) and l (\bullet) as a function of $T \in [298, 373] \text{ K}$. The colored regions indicate the temperatures where the spreads appear as molten, as measured by $\langle R_{2,1} \rangle$. The spread with PO (sample l, $T_M = 327 \text{ K}$) can easily be distinguished from the spread with CB (sample a, $T_M = 317 \text{ K}$) not only by the melting temperature range but also especially by the temperature dependence of $\langle R_{2,2} \rangle$.

3 Results and discussion

3.1 ^1H transverse relaxation of hazelnut-based spreads at 300 MHz

The ^1H magnetization decays were measured at 300 MHz (Figure 3). This NMR spectrometer has a good magnet homogeneity, which allows measuring ^1H spectra with a good line width, i.e., the spectra are spectrally resolved, in contrast to TD-NMR at 20 MHz discussed below in Section 3.2. The magnetization decays were analyzed for the two broad signals, which are superpositions of the NMR signals of different functional groups. It should be noted that the lines are broad, indicating significant homonuclear dipolar couplings, thus obscuring the chemical information. Molecular dynamics averages this dominant spin–spin interaction only partially and is exploited to get access to the quality of the hazelnut-based spreads. A deduction of chemical composition from these ^1H NMR spectra is hardly possible; dilution in an adequate solvent like deuterated chloroform would be needed. Nevertheless, the mean transverse relaxation rates and the corresponding distribution widths can be obtained. Modeling with a bimodal gamma distribution results in two mean relaxation rates $\langle R_{2,1} \rangle$ and $\langle R_{2,2} \rangle$, their distribution widths σ_1 and σ_2 , and amplitudes A_1 and A_2 , which are almost identical and independent of the chemical shift. The analysis of the marked ranges results in identical signal amplitudes within the experimental error. The transverse relaxation depends on the Larmor frequency which is modeled, for example, in the BPP theory (Bloembergen et al., 1948), while the dominant contribution is that of correlation times near the field-independent inverse line width. This circumstance and the above-discussed observations pave the way for TD-NMR. The mq20 low-field instrument, which is suitable and well-established in quality control, can be used to measure the integral transverse

relaxation. This is justified by the analysis of the 300-MHz transverse relaxation measurements and leads to significantly reduced measurement times (Table 3).

3.2 ^1H transverse relaxation of fat and oil reference samples at 20 MHz (TD-NMR)

Transverse relaxation is clearly different for liquid and solid phases of fats, as utilized already in solid fat content (SFC) measurements (Bosin and Marmor, 1968; Mansfield, 1971; Van Putte and Van den Eenden, 1974; IUPAC (International Union of Pure and Applied Chemistry, Commission on Oils, Fats and Derivatives), 1987; International Organization for Standardization ISO 8292, 1991; AOCS Official Methods Cd 16-81, 1993; AOCS Official Methods Cd 16b-93, 1997; Marangoni et al., 2000). Thus, it is possible to distinguish the reference samples contained in spreads, such as the liquid oils HNO, SFO, and RO, from the solid fats PO and CB at room temperature. In addition, the solid–liquid phase transitions of PO and CB can be detected, as shown in the example of the normalized transverse signal decays of CB and PO, measured in the temperature range $T \in [298, 373] \text{ K}$ (Figure 5).

The transverse signal decays cannot be described in a physically meaningful way with a monomodal gamma distribution at $T < T_M$, in contrast to HNO, SFO, and RO. T_M , here defined as the melting temperature, must be known for the fats and the spreads as it shows up in the CPMG measurements. The definition within this paper is as follows: to determine T_M , all data were modeled with a bimodal gamma distribution over the complete temperature range. Subsequently, the amplitude fractions of the two distributions are compared to quantify the temperature transition range characterized by T_M , above which the data are better described by a monomodal gamma distribution, neglecting a small magnetization fraction in the range of 2% (Figure 6). T_M is, thus,

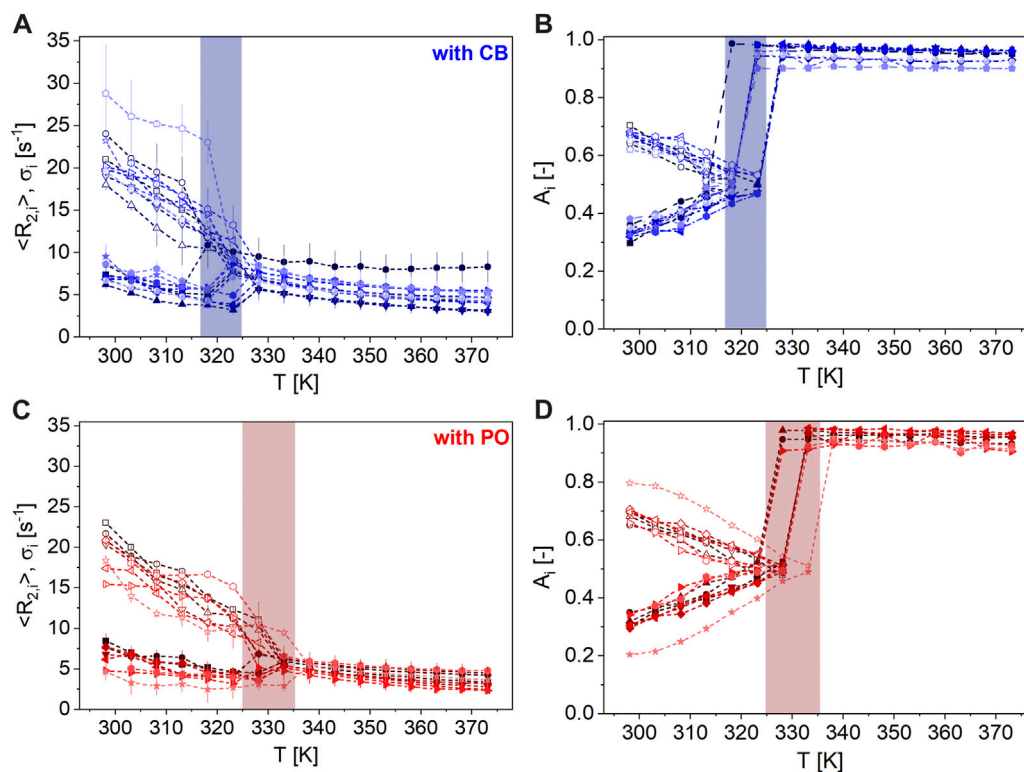


FIGURE 8

(A + C) $\langle R_{2,1} \rangle \in [7, 29] \text{ s}^{-1}$ (unfilled symbols) and $\langle R_{2,2} \rangle \in [2, 10] \text{ s}^{-1}$ (filled symbols) with σ_1 and σ_2 (error bars), respectively, (B + D) A_1 (unfilled symbols) in the range $[0, 80] \%$ and $A_2 = 1 - A_1$ (filled symbols) of the nut spreads with CB (top, blue: sample a (■), b (●), c (▲), d (▼), e (◆), f (◀), g (▶), h (○), i (★), j (⊙), and k (⊕); Table 1) and with PO (bottom, red: sample l (■), m (●), n (▲), o (▼), p (◆), q (◀), r (▶), s (○), and t (★); Table 1) as a function of $T \in [298, 373] \text{ K}$ at 20 MHz. The colored regions indicate the temperature range where all nut spreads with CB (blue, $T_M \in [317, 325] \text{ K}$) and PO (red, $T_M \in [325, 336] \text{ K}$) appear as molten, as deduced from transverse magnetization decays. Nut spreads with CB have a larger dispersion of $\langle R_{2,i} \rangle \in [3, 29] \text{ s}^{-1}$ compared to PO.

defined as the cross-over point of the two amplitudes A_1 and A_2 in this approach.

This approach differs from SFC determination. For the direct SFC determination, the signal amplitude A of an FID is recorded at approximately $10 \mu\text{s}$, directly after the probe's dead time of approximately $6 \mu\text{s}$, and $70 \mu\text{s}$. This leads to the amplitude of the solid $A_S = A(10 \mu\text{s}) - A(70 \mu\text{s})$, while $A(70 \mu\text{s}) = A_L$ is the amplitude of the liquid oil fraction. The corrected ratio of these amplitudes is SFC. SFC is temperature-dependent and already allowed the detection of crystal morphologies of CB and similar fats in combination with well-defined tempering schemes (Pettersson et al., 1985; van Duynhoven et al., 2002). With echo times of 1.2 ms and 2 ms (Table 3), the solid fractions in the sense of SFC are not detected in the current approach of exploring CPMG decays. The approach in this study leads, therefore, to different ranges of melting temperatures and reflects changes in molecular dynamics of the liquid part of SFC (Pettersson et al., 1985). In addition, we observed only the melting of the samples without tempering them along a protocol. All samples were, however, stored at room temperature for weeks before the measurements.

The mean relaxation rates of the faster relaxing components $\langle R_{2,1} \rangle \in [9, 37] \text{ s}^{-1}$ with a larger fraction $A_1 \in [0.52, 0.78]$ of both solid fats CB and PO are considerably larger than the mean relaxation rates $\langle R_2 \rangle \in [2, 11] \text{ s}^{-1}$ of HNO, SFO, and RO for

$T < T_M$. The mean relaxation rates of the slower relaxing components $\langle R_{2,2} \rangle \in [2, 12] \text{ s}^{-1}$ instead are in a similar order of magnitude, indicating the wide spread of molecular fluctuation time scales in these fats. $\langle R_{2,1} \rangle$ of CB and PO could possibly represent the high-melting triglycerides (e.g., 1,3-dipalmitoyl-2-oleoylglycerol (POP)), whereas $\langle R_{2,2} \rangle$ could be assigned to the low-melting triglycerides (e.g., 1,3-dioleoyl-2-palmitoyl glycerol (POO)) in both fats (Müller, 2020; Ghazani and Marangoni, 2021).

HNO, SFO, and RO mainly have a high content of unsaturated fatty acids, i.e., lipophilic molecules in the liquid form at room temperature. The intramolecular, specifically homonuclear dipolar, interactions are time-averaged, leading to long magnetization decays and relatively low relaxation rates in the CPMG experiments. The intrinsic mobility in these fat molecules is larger, i.e., the fluctuations are on a faster time scale than in the structured solids CB and PO in the temperature range observed. At $T = 298 \text{ K}$, CB and PO, both known for their polymorphism, consist of both "liquid" and "solid" triglycerides on the time scale of R_2 . In contrast to HNO, SFO, and RO, the polymorphic crystalline structures in CB and PO influence intrinsic mobility and thus cause faster ^1H transverse relaxation. Thus, $\langle R_2 \rangle$ of HNO, SFO, and RO is smaller than $\langle R_{2,1} \rangle$ of CB and PO for $T < T_M$. In contrast, $\langle R_{2,2} \rangle$ of CB and PO reflects mobile fractions or functional groups, which relax on a time scale similar to HNO, SFO, and RO. As temperature increases, $\langle R_{2,i} \rangle$ decreases, and

TABLE 5 Mean values (M), standard deviations (SD), and minimum (Min) and maximum (Max) values of the mean relaxation rates $\langle R_{2,i} \rangle$, and the corresponding distribution widths σ_i and amplitudes A_i as a function of temperature T for the nut spreads with cocoa butter (A) and with palm oil (B). Melting ranges are $T_M \in [317, 325]$ K for nut spreads with cocoa butter and $T_M \in [325, 336]$ K for nut spreads with palm oil and are marked in color.

A) Nut spreads with cocoa butter																				
T [K]	$\langle R_{2,1} \rangle$ [s^{-1}]				σ_1 [s^{-1}]				$\langle R_{2,2} \rangle$ [s^{-1}]				σ_2 [s^{-1}]				$A_2 = (1-A_1)$ [-]			
	M	SD	Min	Max	M	SD	Min	Max	M	SD	Min	Max	M	SD	Min	Max	M	SD	Min	Max
298	21.2	3.0	18.0	28.8	1.2	3.4	0.0	11.5	7.5	1.0	6.2	9.5	0.8	0.8	0.1	2.8	0.34	0.02	0.30	0.38
303	19.0	2.7	15.6	26.0	1.0	2.6	0.0	8.6	6.5	0.7	5.2	7.6	0.6	0.6	0.1	1.8	0.37	0.02	0.33	0.40
308	17.3	3.1	12.9	25.2	1.8	3.1	0.0	8.4	6.0	1.0	4.3	8.1	0.5	0.6	0.1	1.8	0.39	0.03	0.34	0.44
313	15.7	3.5	10.8	24.6	2.2	2.5	0.0	6.1	5.3	0.8	3.8	6.6	0.7	0.6	0.1	1.8	0.45	0.03	0.39	0.49
318	13.6	3.4	10.5	23.0	3.8	2.2	0.0	6.2	5.3	1.9	3.8	10.9	1.2	1.5	0.1	5.4	0.52	0.16	0.43	0.99
323	8.7	1.3	7.1	11.4	2.3	2.2	0.0	4.7	7.0	2.4	3.2	10.1	2.9	1.6	0.1	4.8	0.81	0.24	0.47	0.98
328	-	-	-	-	-	-	-	-	7.1	1.1	5.6	9.5	3.1	0.6	2.4	4.4	0.96	0.03	0.90	0.99
333	-	-	-	-	-	-	-	-	6.6	1.1	5.1	8.8	2.9	0.6	2.1	4.1	0.95	0.03	0.90	0.98
338	-	-	-	-	-	-	-	-	6.1	1.2	4.7	8.9	2.6	0.6	1.9	4.2	0.95	0.02	0.91	0.98
343	-	-	-	-	-	-	-	-	5.7	1.1	4.3	8.3	2.4	0.6	1.7	3.8	0.95	0.02	0.90	0.97
348	-	-	-	-	-	-	-	-	5.5	1.2	4.0	8.3	2.3	0.6	1.5	3.7	0.95	0.02	0.91	0.97
353	-	-	-	-	-	-	-	-	5.2	1.2	3.7	8.0	2.1	0.6	1.4	3.6	0.94	0.03	0.90	0.97
358	-	-	-	-	-	-	-	-	5.0	1.2	3.6	8.0	2.1	0.6	1.4	3.6	0.94	0.03	0.90	0.97
363	-	-	-	-	-	-	-	-	4.9	1.3	3.3	8.1	2.1	0.7	1.2	3.7	0.94	0.03	0.90	0.97
368	-	-	-	-	-	-	-	-	4.8	1.4	3.2	8.2	2.0	0.7	1.1	3.7	0.94	0.03	0.90	0.97
373	-	-	-	-	-	-	-	-	4.7	1.4	3.0	8.3	2.0	0.8	1.0	3.8	0.94	0.02	0.90	0.96
B) Nut spreads with palm oil																				
T [K]	$\langle R_{2,1} \rangle$ [s^{-1}]				σ_1 [s^{-1}]				$\langle R_{2,2} \rangle$ [s^{-1}]				σ_2 [s^{-1}]				$A_2 = (1-A_1)$ [-]			
	M	SD	Min	Max	M	SD	Min	Max	M	SD	Min	Max	M	SD	Min	Max	M	SD	Min	Max
298	19.9	2.4	15.4	23.0	0.3	0.4	0.0	1.2	6.6	1.3	4.7	8.4	1.1	0.7	0.1	2.0	0.31	0.05	0.20	0.38
303	17.9	2.0	14.0	20.3	0.5	0.6	0.0	1.6	5.9	1.3	3.2	7.0	1.3	1.1	0.1	3.2	0.34	0.05	0.21	0.40
308	15.9	1.9	11.8	18.7	0.7	1.1	0.0	3.1	5.2	1.0	2.9	6.5	1.2	1.1	0.1	3.6	0.37	0.05	0.25	0.44
313	14.6	2.2	11.3	17.4	1.0	1.5	0.0	4.2	4.8	1.0	3.1	6.4	0.9	0.7	0.1	1.9	0.41	0.05	0.29	0.47
318	13.2	2.5	9.6	17.2	0.9	1.5	0.0	4.4	4.3	0.8	2.4	5.2	1.1	1.1	0.1	3.2	0.44	0.04	0.35	0.49
323	11.1	1.9	8.3	15.1	1.4	1.8	0.1	4.5	4.3	1.5	2.7	8.3	1.3	1.2	0.1	3.9	0.52	0.15	0.40	0.93
328	8.8	2.2	5.1	11.1	2.6	1.7	0.1	4.9	4.9	1.7	3.1	7.9	1.7	1.2	0.1	3.8	0.68	0.23	0.46	0.98
333	6.3	1.6	5.1	9.5	2.1	0.5	1.0	2.5	5.6	1.2	2.9	7.1	2.4	0.5	1.4	3.3	0.91	0.15	0.49	0.99
338	-	-	-	-	-	-	-	-	5.3	0.7	4.2	6.6	2.2	0.4	1.8	3.0	0.95	0.02	0.91	0.98
343	-	-	-	-	-	-	-	-	4.9	0.8	3.7	6.3	2.0	0.4	1.7	2.7	0.95	0.03	0.91	0.98
348	-	-	-	-	-	-	-	-	4.6	0.8	3.4	6.2	1.9	0.4	1.5	2.8	0.95	0.02	0.91	0.98
353	-	-	-	-	-	-	-	-	4.4	0.9	3.0	5.9	1.7	0.4	1.3	2.6	0.95	0.02	0.90	0.98
358	-	-	-	-	-	-	-	-	4.1	0.9	2.7	5.8	1.6	0.5	1.2	2.6	0.95	0.02	0.90	0.98
363	-	-	-	-	-	-	-	-	3.9	1.0	2.5	5.7	1.5	0.5	1.0	2.6	0.94	0.03	0.90	0.98
368	-	-	-	-	-	-	-	-	3.8	1.0	2.4	5.4	1.5	0.5	0.9	2.5	0.94	0.02	0.91	0.97
373	-	-	-	-	-	-	-	-	3.6	1.1	2.3	5.5	1.4	0.6	0.8	2.6	0.94	0.03	0.90	0.97

In the original version, the lines of the transition temperatures were marked in color (A) for cocoa butter T = 318 and 323 K, blue and (B) for palm oil T = 328 and 333 K, red.

the amplitude proportions of faster and slower relaxing components in CB and PO, reflecting temperature-dependent melting, change.

$\langle R_{2,1} \rangle = 37 \text{ s}^{-1}$ of CB is larger than $\langle R_{2,1} \rangle = 29 \text{ s}^{-1}$ of PO at $T = 298 \text{ K}$. $\langle R_{2,1} \rangle$ decreases steadily with temperature for CB, whereas the decrease in $\langle R_{2,1} \rangle$ of PO, reflecting the transition from a solid to a liquid phase, is observed over a wider temperature range. Thus, melting as monitored by TD-NMR CPMG is determined for CB at $T_M = 314 \text{ K}$, for PO at $T_M = 324 \text{ K}$. This reflects the multiscale properties of fats and is consistent with other studies, for example, Sonwai et al. (2014), Nikolaeva et al. (2018), and Nikolaeva et al. (2019) and references therein. At $T > T_M$, i.e., in the liquid state, transverse relaxation occurs on a similar time scale for all measured reference samples. Due to the different characteristics of triglyceride compositions of CB and PO, the fats do not have well-defined melting temperatures but melting temperature ranges which are additionally strongly influenced by the polymorphism of the respective fat crystals (Garti and Sato, 2001; Chong et al., 2007). Different triglycerides of PO with their respective different melting ranges allow diverse fractions to be obtained from PO (Omar et al., 2015; Yilmaz and Ağagündüz, 2022). The two best-known products of fractionation are palm olein and palm stearin. Fractionation allows one to separate oils or fats with different physical properties and mix them in specific ratios to produce products such as nut spreads with defined phase transition ranges. For example, a higher proportion of palm stearin can give the product a higher $T_M = 325 \text{ K}$ (Hubbes et al., 2020). In addition, the time scales of tempering and of observation, i.e., the analytical method, need to be considered when defining a solid–liquid phase transition.

3.3 ^1H transverse relaxation of hazelnut-based spreads at 20 MHz (TD-NMR)

Hazelnut-based spreads can be classified into spreads with CB or with PO when considering fat composition, as indicated on the packaging. The measurements on two representative nut spreads with CB (sample a, Table 1) and PO (sample l, Table 1) result in the temperature dependence of transverse relaxation shown in Figure 7. The low-temperature magnetization decays need to be modeled by bimodal gamma distributions, while at $T > 330 \text{ K}$, similar behavior is observed, as for the reference samples CB and PO (Figure 7). This similarity led to the conclusion that the melting of these two fats is mainly observed as changes in magnetization decays when measuring CPMG on the spreads as a function of temperature in the range [298, 373] K. Monomodal distributions describe the data sufficiently for $T > T_M$, and the cross-points of the amplitudes can be defined according to the previous definition. This leads to $T_M = 317 \text{ K}$ in the case of sample a and to $T_M = 327 \text{ K}$ for sample l.

This difference is explored in the following for other commercially available nut spreads to prove the reliability of the approach and to get an estimate of the span of the values within the two classes of hazelnut-based spreads: Eleven hazelnut-based spreads with CB are compared to nine samples with PO, regarding their transverse relaxation behavior (Figure 8). When collecting the samples, special emphasis was placed on the maximal variation of ingredients and of origin to sense the span width of transverse relaxation of commercially available hazelnut-based spreads.

At $T < T_M$, bimodal distributions describe the measured magnetization decays numerically very well, while above T_M , a monomodal distribution leads to relaxation rates in the order of the reference oils. Spreads with CB show a pronounced decrease in $\langle R_{2,1} \rangle$ in the temperature range $T_M \in [317, 325] \text{ K}$, whereas spreads with PO show a decrease at higher temperatures $T_M \in [325, 336] \text{ K}$. Common to all of them is that T_M values of spreads are larger than those of the reference samples, which is attributed to the presence of solid components and the composition detailed in Table 1.

Since spreads are multicomponent systems (Table 1), the observation is in line with findings on other materials and is caused by interactions between different ingredients, leading to changes in the microscopic structure, which affect R_2 . The critical temperature range marked in Figure 8 depends on the fat type and content, sugar content, and other ingredients, especially solid particles like fibers, crunchies, and pieces of chocolate. The higher T_M value of spreads containing PO is in line with the finding on PO. Furthermore, the scatter in T_M of different nut spreads can be attributed to different triglyceride compositions by fractionation; a wider T_M range is, therefore, expected.

A larger dispersion of the relaxation values $\langle R_{2,i} \rangle \in [3, 29] \text{ s}^{-1}$ was measured for nut spreads with CB. It is possible that the faster $\langle R_{2,i} \rangle$ is related to a higher content of solid components contained therein, such as dried rice syrup or dietary fiber, or a low addition of clarified butter, for example, spread j. The hazelnut-based spreads containing PO show a larger span-width in the amplitudes, which is mainly due to sample t with a white–brown pattern in the spread. This indicates that the coloring agent defatted cocoa powder also plays a major role in transverse relaxation at $T < T_M$. Despite large recipe variations, it, nevertheless, is possible to distinguish spreads with PO or CB via transverse relaxation with TD-NMR. As a supplement to Figure 8, Table 5 shows the mean values (M), standard deviations (SD), and minimum (Min) and maximum (Max) values of the respective parameters of the data analysis as a function of temperature.

The difference in the transverse relaxation behavior as a function of T provides the basis for an SOP to characterize hazelnut-based spreads in the sense of quality control and to detect frauds:

- 1) Sensitive low-field NMR spectrometer capable of ^1H multi-echo detection in a temperature range $T \in [253, 353] \text{ K}$, preferentially equipped with a 10-mm probe and a cylindrical sensitive region of 10 mm height.
- 2) Sample preparation: Conventional 10-mm glass tubes are filled with the spread up to a filling level of 10 mm for defined rf-pulse properties and decently homogeneous temperature within the sample volume. To avoid smearing over the whole NMR tube, two approaches can be used: one approach is applied where the spread is extracted from the package using a plastic or metal tube with an outer diameter smaller than the inner diameter of the NMR tube. The spread is pulled out into the NMR tube by either pressurized air or mechanically by a stamp fitting into the plastic or metal tube. The alternative is to use a dedicated cylindrical vial with an outer diameter of <10 mm and a height of <20 mm. The small sample-containing vial is placed into the NMR instrument with a dedicated holder, preferentially equipped with a thread for a

stable connection to the vial and made of a material with low heat capacity and small diameter for minimal temperature gradients.

- 3) The sample is placed into the instrument. The sample chamber is at the lowest temperature when starting the analysis. The sample is kept for a minimum of 10 min at that temperature in the NMR instrument, the NMR pulse sequence parameters and the matching of the NMR probe are checked, and finally, the measurement is determined.
- 4) Data processing needs to be done with either the inverse Laplace transform or with a mathematic analytical distribution model as the preferred gamma model described above.
- 5) T -dependent measurements are performed, and the relaxation rates are plotted, including the distribution width as a function of T . The steepest slope and change of the magnetization decays are deduced, and it is compared with values of known hazelnut-based spreads according to the procedure described above.
- 6) The thus determined melting temperature allows the classification of the measured spread as mainly based on CB ($T_M < 325$ K) and PO ($T_M > 325$ K).

The method was found to work reliably for commercially available hazelnut-based spreads. Deviations occur and are expected for spreads containing other oils and fats and of drastically different compositions. For example, almond-containing spreads show a different melting behavior and need, therefore, a separate treatment.

4 Conclusion

Transverse relaxation was measured by TD-NMR, which was justified by comparative measurements on a 300 MHz NMR with a spectral resolution revealing unique relaxation over the chemical shift range. TD-NMR, thereby, has the advantages of being relatively simple and comparable low costs in investment and maintenance, which makes a dedicated application suitable for industrial application in quality control and fraud detection.

Cocoa butter and palm oil can be distinguished by transverse relaxation, even in more complex recipes of spreads containing solid fractions or inhomogeneously distributed defatted cocoa powder. Care should be taken regarding the choice of temperatures that need to be scanned to obtain a reliable evaluation of the spread under investigation.

From the scientific point of view, the results show that the main components which cause the steep change in relaxation as a function of temperature are the two named fats, while the other ingredients are not neglectable but determine the span-width, especially in the temperature range below the melting temperature range. Further investigation will consider the impact of palm oil fractionation and of other oils, almonds, or peanuts, which were excluded in the present study.

Author's note

The responsibility for the content of this publication lies with the authors.

Data availability statement

The raw data supporting the conclusion of this article will be made available by the authors, without undue reservation.

Author contributions

LT: conceptualization, data curation, formal analysis, investigation, methodology, project administration, software, supervision, validation, visualization, writing–original draft, and writing–review and editing. SK: data curation, investigation, and writing–review and editing. HS: writing–review and editing. HN: funding acquisition, resources, and writing–review and editing. GG: conceptualization, data curation, formal analysis, funding acquisition, investigation, methodology, project administration, resources, software, supervision, validation, visualization, writing–original draft, and writing–review and editing.

Funding

The authors declare that financial support was received for the research, authorship, and/or publication of this article. This research was funded by the German Federal Ministry of Economic Affairs and Climate Action (BMWK) through the program to promote collective industrial research (IGF) with the German Federation of Industrial Research Association (AiF), IGF-Nr. 21785 N. The Deutsche Forschungsgemeinschaft (DFG) is acknowledged for the substantial financial contribution in form of NMR instrumentation and within the instrumental facility Pro²NMR.

Acknowledgments

The authors thank the German Federation of Industrial Research Association (AiF) and the Deutsche Forschungsgemeinschaft (DFG) for financial support.

Conflict of interest

The authors declare that the research was conducted in the absence of any commercial or financial relationships that could be construed as a potential conflict of interest.

Publisher's note

All claims expressed in this article are solely those of the authors and do not necessarily represent those of their affiliated organizations, or those of the publisher, the editors, and the reviewers. Any product that may be evaluated in this article, or claim that may be made by its manufacturer, is not guaranteed or endorsed by the publisher.

References

- AOCS Official Methods Cd 16-81 (1993). *Solid fat content (SFC) by low-resolution nuclear magnetic resonance, indirect and direct methods*.
- AOCS Official Methods Cd 16b-93 (1997). *Solid fat content (SFC) by low-resolution nuclear magnetic resonance, indirect and direct methods*.
- Aydemir, O. (2019). Utilization of different oils and fats in cocoa hazelnut cream production. *J. Food Process. Preserv.* 43 (5), e13930. doi:10.1111/jfpp.13930
- Bloembergen, N., Purcell, E. M., and Pound, R. V. (1948). Relaxation effects in nuclear magnetic resonance absorption. *Phys. Rev.* 73 (7), 679–712. doi:10.1103/physrev.73.679
- Blümich, B. (2019). Low-field and benchtop NMR. *J. Magnetic Reson.* 306, 27–35. doi:10.1016/j.jmr.2019.07.030
- Bosin, W. A., and Marmor, R. A. (1968). The determination of the solids content of fats and oils by nuclear magnetic resonance. *J. Am. Oil Chemists' Soc.* 45 (5), 335–337. doi:10.1007/BF02667105
- Chong, C. L., Kamarudin, Z., Lesieur, P., Marangoni, A., Bourgaux, C., and Ollivon, M. (2007). Thermal and structural behaviour of crude palm oil: crystallisation at very slow cooling rate. *Eur. J. Lipid Sci. Technol.* 109 (4), 410–421. doi:10.1002/ejlt.200600249
- Chowdhury, K., Banu, L. A., Khan, S., and Latif, A. (2007). Studies on the fatty acid composition of edible oil. *Bangladesh J. Sci. Industrial Res.* 42 (3), 311–316. doi:10.3329/bjsir.v42i3.669
- Cordella, C., Moussa, I., Martel, A.-C., Sbirrazzuoli, N., and Lizzani-Cuvellier, L. (2002). Recent developments in food characterization and adulteration detection: technique-oriented perspectives. *J. Agric. food Chem.* 50 (7), 1751–1764. doi:10.1021/jf011096z
- Crews, C., Hough, P., Godward, J., Brereton, P., Lees, M., Guet, S., et al. (2005). Study of the main constituents of some authentic hazelnut oils. *J. Agric. food Chem.* 53 (12), 4843–4852. doi:10.1021/jf047836w
- Díaz, M. F., Gavin Szatornil, J. A., Ledea, O., Hernández, F., Alaiz, M., and Garcés, R. (2005). Spectroscopic characterization of ozonated sunflower oil. *Ozone Sci. Eng.* 27 (3), 247–253. doi:10.1080/01919510590945822
- Ezeanaka, M. C., Nsor-Atindana, J., and Zhang, M. (2019). Online low-field nuclear magnetic resonance (LF-NMR) and magnetic resonance imaging (MRI) for food quality optimization in food processing. *Food Bioprocess Technol.* 12, 1435–1451. doi:10.1007/s11947-019-02296-w
- Förster, E., Nirschl, H., and Guthausen, G. (2017). NMR diffusion and relaxation for monitoring of degradation in motor oils. *Appl. Magn. Reson.* 48 (1), 51–65. doi:10.1007/s00723-016-0842-0
- Garti, N., and Sato, K. (2001). *Crystallization processes in fats and lipid systems*. Boca Raton: CRC Press.
- Ghazani, S. M., and Marangoni, A. G. (2021). Molecular origins of polymorphism in cocoa butter. *Annu. Rev. Food Sci. Technol.* 12, 567–590. doi:10.1146/annurev-food-070620-022551
- Hills, B. P. (2006). "Applications of low-field NMR to food science," in *Annual reports on NMR spectroscopy*. Editor G. A. Webb (Academic Press), 177–230.
- Hubbes, S.-S., Braun, A., and Foerst, P. (2020). Crystallization kinetics and mechanical properties of nougat creme model fats. *Food Biophys.* 15 (1), 1–15. doi:10.1007/s11483-019-09596-w
- International Organization for Standardization ISO 8292 (1991). *Animal and vegetable fats and oils—determination of solid fat content—pulsed nuclear magnetic resonance method*.
- IUPAC (International Union of Pure and Applied Chemistry, Commission on Oils, Fats and Derivatives) 2.150 (1987). *Solid content determination in fats by NMR (low resolution nuclear magnetic resonance)*.
- Kovács, A., Körmendi, L., and Kerti, K. B. (2021). Palm oil substitution in hazelnut spread. *Prog. Agric. Eng. Sci.* 17, 111–117. doi:10.1556/446.2021.30013
- Lewinska, A., Zebrowski, J., Duda, M., Gorka, A., and Wnuk, M. (2015). Fatty acid profile and biological activities of linseed and rapeseed oils. *Molecules* 20 (12), 22872–22880. doi:10.3390/molecules201219887
- Mansfield, P. B. (1971). A new wide-line NMR analyzer and its use in determining the solid-liquid ratio in fat samples. *J. Am. Oil Chemists' Soc.* 48 (1), 4–6. doi:10.1007/BF02673231
- Marangoni, A. G., Wright, A. J., Narine, S. S., and Lencki, R. W. (2000). Comment on the use of direct pulsed nuclear magnetic resonance solid fat content measurements in phase behavior studies of lipid mixtures. *J. Am. Oil Chem. Soc.* 77 (5), 565–567. doi:10.1007/s11746-000-0090-9
- Marra, F., Lavorgna, A., Incarnato, L., Malvano, F., and Albanese, D. (2023). Optimization of hazelnut spread based on total or partial substitution of palm oil. *Foods* 12 (16), 3122. doi:10.3390/foods12163122
- Meiboom, S., and Gill, D. (1958). Modified spin-echo method for measuring nuclear relaxation times. *Rev. Sci. Instrum.* 29 (8), 688–691. doi:10.1063/1.1716296
- Meyer, K., Kern, S., Zientek, N., Guthausen, G., and Maiwald, M. (2016). Process control with compact NMR. *TrAC Trends Anal. Chem.* 83, 39–52. doi:10.1016/j.trac.2016.03.016
- Müller, M. T. (2020). *Einfluss freier Fettsäuren auf die kristallisationskinetischen und polymorphen Eigenschaften von Kakaobutter und -äquivalenten*. Göttingen: Cuvillier Verlag.
- Naik, B., and Kumar, V. (2014). Cocoa butter and its alternatives: a review. *J. Bioresour. Eng. Technol.* 1, 7–17.
- Nikolaeva, T., den Adel, R., van der Sman, R., Martens, K. J. A., Van As, H., Voda, A., et al. (2019). Manipulation of recrystallization and network formation of oil-dispersed micronized fat crystals. *Langmuir* 35 (6), 2221–2229. doi:10.1021/acs.langmuir.8b03349
- Nikolaeva, T., Den Adel, R., Velichko, E., Bouwman, W., Hermida-Merino, D., Van As, H., et al. (2018). Networks of micronized fat crystals grown under static conditions. *Food & Funct.* 9 (4), 2102–2111. doi:10.1039/C8FO00148K
- Ogrinc, N., Košir, I. J., Spangenberg, J. E., and Kidrič, J. (2003). The application of NMR and MS methods for detection of adulteration of wine, fruit juices, and olive oil. A review. *Anal. Bioanal. Chem.* 376 (4), 424–430. doi:10.1007/s00216-003-1804-6
- Omar, Z., Hishamuddin, E., Mat Sahri, M., Hazirah, S., Lida, N., Roddy Ramli, M., et al. (2015). Palm oil crystallisation: a review. *J. Oil Palm Res.* 27 (2), 97–106.
- Petersson, B., Anjou, K., and Sandström, L. (1985). Pulsed NMR method for solid fat content determination in tempering fats, Part I: cocoa butters and equivalents. *Fette, Seifen, Anstrichm.* 87 (6), 225–230. doi:10.1002/lipi.19850870603
- Principato, L., Carullo, D., Duserm Garrido, G., Bassani, A., Dordoni, R., and Spigno, G. (2022). Rheological and tribological characterization of different commercial hazelnut-based spreads. *J. Texture Stud.* 53 (2), 196–208. doi:10.1111/jtxs.12655
- Santos, P. M., Kock, F. V. C., Santos, M. S., Lobo, C. M. S., Carvalho, A. S., and Colnago, L. A. (2017). Non-invasive detection of adulterated olive oil in full bottles using time-domain NMR relaxometry. *J. Braz. Chem. Soc.* 28, 385–390. doi:10.5935/0103-5053.20160188
- Santos, P. M., Pereira, E. R., and Colnago, L. A. (2016). Detection and quantification of milk adulteration using time domain nuclear magnetic resonance (TD-NMR). *Microchem. J.* 124, 15–19. doi:10.1016/j.microc.2015.07.013
- Siddiqui, A. J., Musharraf, S. G., Choudhary, M. I., and Rahman, A. U. (2017). Application of analytical methods in authentication and adulteration of honey. *Food Chem.* 217, 687–698. doi:10.1016/j.foodchem.2016.09.001
- Sonwai, S., Kaphueakngam, P., and Flood, A. (2014). Blending of mango kernel fat and palm oil mid-fraction to obtain cocoa butter equivalent. *J. food Sci. Technol.* 51, 2357–2369. doi:10.1007/s13197-012-0808-7
- Trapp, L., Schacht, H., Eymann, L., Nirschl, H., and Guthausen, G. (2023). Oil mobility in hazelnut oil-based oleogels investigated by NMR. *Appl. Magn. Reson.* 54, 1445–1462. doi:10.1007/s00723-023-01571-6
- Ulberth, F., and Buchgraber, M. (2000). Authenticity of fats and oils. *Eur. J. Lipid Sci. Technol.* 102 (11), 687–694. doi:10.1002/1438-9312(200011)102:11<687::AID-EJLT687>3.0.CO;2-F
- van Duynhoven, J., Dubourg, I., Goudappel, G. J., and Roijers, E. (2002). Determination of MG and TG phase composition by time-domain NMR. *J. Am. Oil Chem. Soc.* 79 (4), 383–388. doi:10.1007/s11746-002-0493-7
- van Duynhoven, J., Voda, A., Witek, M., and Van As, H. (2010). Time-domain NMR applied to food products. *Annu. Rep. NMR Spectrosc.* 69, 145–197. doi:10.1016/S0066-4103(10)69003-5
- Van Putte, K. P., and Van den Eenden, J. (1974). Fully automated determination of solid fat content by pulsed NMR. *J. Am. Oil Chem. Soc.* 51 (7), 316–320. doi:10.1007/BF02633005
- World Bank (2023). *Monatlicher importpreis von Palmöl in europa von Januar 2014 bis september 2023 (in US-dollar pro tonne)*. Statista.
- Yılmaz, B., and Ağagündüz, D. (2022). Fractionated palm oils: emerging roles in the food industry and possible cardiovascular effects. *Crit. Rev. food Sci. Nutr.* 62 (7), 1990–1998. doi:10.1080/10408398.2020.1869694